

The Kerr effect in aqueous dispersions of anisotropic and electrically charged latex particles

This article has been downloaded from IOPscience. Please scroll down to see the full text article.

1992 J. Phys.: Condens. Matter 4 8683

(<http://iopscience.iop.org/0953-8984/4/45/004>)

View [the table of contents for this issue](#), or go to the [journal homepage](#) for more

Download details:

IP Address: 171.66.16.96

The article was downloaded on 11/05/2010 at 00:48

Please note that [terms and conditions apply](#).

The Kerr effect in aqueous dispersions of anisotropic and electrically charged latex particles

F Mantegazza, M Giardini, R Piazza and V Degiorgio

Dipartimento di Elettronica – Sezione di Fisica Applicata, Università di Pavia, 27100 Pavia, Italy

Received 29 April 1992, in final form 20 July 1992

Abstract. Static and dynamic electric birefringence measurements are performed on dispersions of electrically charged fluorinated latex spheres. It is shown that the Kerr constant is made up of three contributions: the first depends on the intrinsic and form anisotropy of the particle; the second arises from the presence of a slowly fluctuating electric dipole which should be originated by the statistics of the surface charge distribution, and the third is connected with the cloud of dissociated counter-ions. This latter contribution shows a non-Lorentzian frequency dispersion, and its amplitude is strongly dependent on the particle concentration and on the ionic strength.

1. Introduction

The electric birefringence behaviour of polyelectrolyte aqueous solutions is complex and only partially understood [1–11]. The presence of mobile charges makes polyelectrolyte solutions strongly electrically active: both the Kerr constant and the dielectric constant [12] of the solution may become quite large even at low polyelectrolyte concentrations. Transient electric birefringence (TEB) studies can give important information on the dielectric properties of the solution, mainly because they allow easy separation of contributions due to different physical mechanisms.

Several TEB experiments were performed using both rigid particles with simple geometrical shapes [1–4], and flexible polyelectrolytes [5–11]. In the case of Tobacco Mosaic Virus (TMV) solutions, the available data [1–3] indicate the presence of two distinct dielectric relaxations, one with a cut-off frequency of a few hundred Hz and the other with a cut-off frequency around 30 kHz. The molecular mechanisms have not been fully clarified as yet. Concerning the low-frequency relaxation, some authors [2, 3] have invoked the existence of a permanent electric dipole, but the structure of the used macromolecules or colloidal particles is such that there is no reason to expect a permanent dipole. Concerning the high-frequency relaxation, various explanations involving the role of counter-ion polarization have been proposed [1, 12]. We have recently performed a study of aqueous dispersions of charged rod-like latex particles [4], and we have found that the amplitude of the contribution showing the high-frequency relaxation is mainly, if not completely, due to interparticle interactions, whereas the previous papers were describing it in terms of a single-particle property.

Effects similar to those observed with TMV solutions have also been found in TEB experiments on flexible polyelectrolytes, like DNA [5] and sodium polystyrene

sulphonate (Napss) [6–11]. The interpretation is even more complicated than for rigid particles because flexible polyelectrolytes present a statistical configuration which changes when some experimental parameters, like the ionic strength or the polyelectrolyte concentration, are varied.

In order to get a clearer picture, it is helpful to study first a simple system made up of monodisperse rigid macro-ions. We have recently investigated in detail, by using static and dynamic light scattering [13], aqueous dispersions of fluorinated latex particles which are made from a polytetrafluoroethylene copolymer (PFA). It was found that the PFA particles are rather monodisperse and quasi-spherical, have an index of refraction close to that of water and possess an intrinsic optical anisotropy. They are, therefore, a very interesting model system for a TEB study of the dielectric properties of polyelectrolytes. We present in this paper a transient electric birefringence experiment performed with aqueous dispersions of these latex particles. By measuring the response to the applied electric field both in the time and frequency domain, we are able to distinguish three distinct contributions to the Kerr constant. The first has an electronic origin and does not depend on the frequency of the applied field, the second appears only at low frequencies and is due to the presence of charged sites and bound (but mobile) counter-ions on the particle surface, the third is strongly dependent on the particle volume fraction and on the concentration of added salt and is presumably connected with the dynamics of the clouds of non-associated counter-ions and with the interactions among clouds belonging to different particles. The frequency dispersion of the third contribution is markedly different from a Lorentzian shape, and fits the theoretical prediction for the frequency dependence of the dielectric constant of a dispersion of spherical polyelectrolytes very well.

2. Experimental results

We have used an aqueous dispersion of nearly monodisperse latex particles of an alkoxyvinylether-tetrafluoroethylene copolymer (PFA, commercially known as Hyflon) obtained from Montefluos SpA, Spinetta Marengo (Italy). The shape of the particles is close to spherical, as shown by the electron microscope picture of figure 1. The particles have an average index of refraction, $n_p = 1.352$, close to that of water, and present an appreciable intrinsic optical anisotropy, which derives from their partially crystalline internal structure [13]. By assuming that the particles possess an optical axis, we have derived the anisotropy of the refractive index, $\delta n_{\text{int}} = n_1 - n_2 = 0.0051$, where the index 1 refers to the direction parallel to the symmetry axis of the particle, and the index 2 to any direction perpendicular to the symmetry axis.

The experiment was performed on particles with radius $R = 90$ nm at volume fractions Φ ranging from 10^{-3} to 2.5×10^{-2} . The original latex ($\Phi \approx 20\%$) was dialyzed for some weeks until its conductivity reached a stable value of about $100 \mu\text{S cm}^{-1}$, and then diluted with a small quantity of non-ionic surfactant added to prevent any coagulation. Some measurements were performed by adding NaCl to the solution in order to investigate the dependence of the response on the ionic strength. A general description of our optical and detection apparatus can be found in [14]. The TEB experiment [15–18] essentially consists of applying a rectangular voltage pulse to the electrodes of the Kerr cell, with a pulse duration long enough to reach a stationary value of the induced anisotropy, and of observing the relaxation

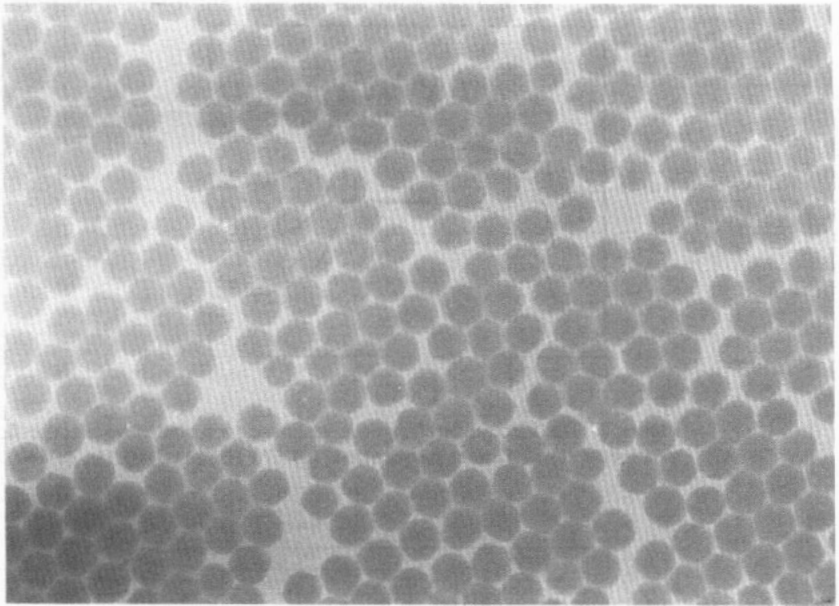


Figure 1. A transmission electron microscope picture of the PFA latex particles.

of the induced birefringence after the electric field is switched off. In most of the measurements that are discussed here the applied electric field consisted of a sine-wave pulse of zero average and frequency variable between 100 Hz and 2 MHz. The pulse was obtained by gating a function generator and amplifying the output with a Krohn-Hite 7500 power amplifier. The pulse duration was in the range 1–10 ms. Sine-wave pulses of variable frequency and zero time average allow, at the same time, the avoidance of steady-state electric currents in the cell and the singling out of the contribution of distinct polarization mechanisms at different frequencies. In some cases we also used a classical reversing pulse technique. The birefringence signal is obtained by putting the Kerr cell between two polarizers (with the insertion of a quarter-wave plate between cell and analyser) and by sending a laser beam through the optical system. Signal averaging over many pulses was performed by Data Precision DATA 6100 digital oscilloscope. All the reported results were obtained in the Kerr regime where the induced birefringence Δn is proportional to the square of the electric field E . The Kerr constant is defined as $B = \Delta n / (\lambda E^2)$, where λ is the wavelength of the laser beam. In our experiment, $\lambda = 0.633 \mu\text{m}$.

The electric birefringence response to a sinusoidal field consists of a DC component plus a sinusoidal component oscillating at twice the frequency ν of the exciting signal [3]. Some of the observed transients are presented in figure 2. The amplitude of the sinusoidal component is a decreasing function of ν . After the applied electric field is switched off, the induced birefringence decays exponentially (see figure 3), with a decay constant τ_r which does not depend on the frequency of the applied field. We obtain from our data $\tau_r = (605 \pm 20) \mu\text{s}$, in good agreement with the expression for the rotational diffusion time constant, $\tau_r = 4\pi\eta R^3 / (3k_B T)$, where η is the viscosity of the solvent, k_B the Boltzmann constant and T the absolute temperature. As expected [3], the observed cut-off frequency for the amplitude of

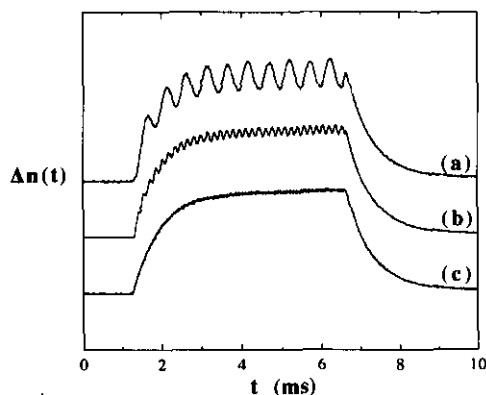


Figure 2. The electric birefringence response to a sine-wave electric field pulse of zero average at three distinct frequencies: (a) 970 Hz, (b) 3100 Hz, (c) 44000 Hz.

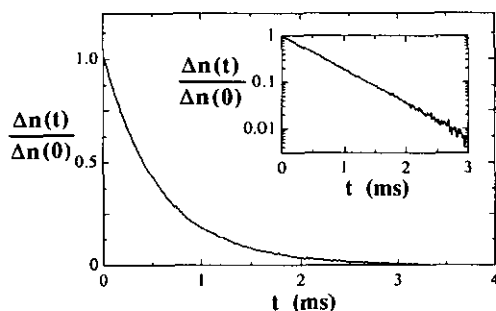


Figure 3. The exponential decay of the pulses shown in figure 2. The inset shows a semi-logarithmic plot.

the sinusoidal component is around $(6\pi\tau_r)^{-1}$.

We have studied dispersions with concentrations of added NaCl, c_s , in the range 0–5 mM. Dispersions without added salt have an electric conductivity in the range of a few $\mu\text{S cm}^{-1}$, which is much larger than that expected from the particle counter-ions alone and is mainly due to the carbon dioxide dissolved in water.

In all cases, the decay of the induced birefringence pulse is found to be exponential, with a decay constant coinciding with τ_r . This means that, in all the investigated situations, electrostatic interactions have little effect on the rotational Brownian motion of the individual particle.

We report in figure 4 the specific Kerr constant B/Φ , derived from the steady-state DC component, as a function of the frequency ν of the exciting wave, at various volume fractions Φ . All the data of figure 4 were obtained at $c_s = 0.2$ mM. We note that the Kerr constant is positive. The amplitude of the frequency-dependent contribution to B/Φ grows with Φ , leaving the shape of the frequency response substantially unchanged, which presents a cut-off frequency of around 30 kHz. As shown in figure 5, the amplitude of such a contribution is a rapidly decreasing function of the ionic strength, becoming negligible when c_s exceeds 5 mM. The dependence of B/Φ on Φ at $c_s = 0.2$ mM is shown in figure 6 for two distinct frequencies of

the applied field: at $\nu = 2.5$ kHz, B/Φ increases linearly with Φ in the range of investigated volume fractions. At $\nu = 1$ MHz, B/Φ becomes independent of Φ , and takes the value $(0.90 \pm 0.05) \times 10^{-8} \text{ mV}^{-2}$.

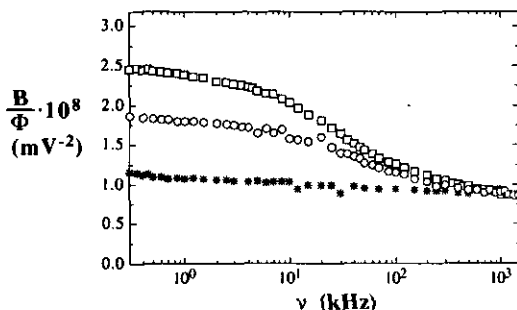


Figure 4. The specific Kerr constant measured as a function of the frequency of the electric field, at $c_s = 0.2$ mM, for three distinct volume fractions: *, $\Phi = 0.1\%$; O, $\Phi = 1\%$; □, $\Phi = 2.5\%$.

In order to check the dependence of the high-frequency value of B/Φ on the mismatch in refractive index between particle and solvent, we have measured B at $\Phi = 1\%$ and $\nu = 1$ MHz in a mixed water-glycerol solvent. The results are shown in figure 7. The refractive index of the solvent, n_s , ranges from 1.333 for pure water to 1.364 for the mixture containing 25% by weight of glycerol. We see that B is almost insensitive to the optical mismatch between particle and solvent.

When the frequency of the applied field is very low (say, below 200 Hz), it is possible to notice an additional contribution to B/Φ . However, it is rather difficult to obtain reliable data at very low frequencies by using sinusoidal fields, because of electrode polarization effects, so we have chosen to study this slow contribution by working in the time domain with the reversing-pulse technique. The technique consists of applying a field pulse, and then suddenly reversing the field direction [16]. We show in figure 8 the transient observed with a 0.1% dispersion, the transient presents a dip after field reversal. The amplitude of the dip is about 30% of the total amplitude of the TEB signal. A close analysis of the transient also reveals that the rise of the transient is slower than the decay. We have found that the shape of the transient is not appreciably modified by the addition of the NaCl up to 3 mM at fixed Φ . By increasing Φ at low ionic strength, the dip becomes fractionally smaller.

3. Discussion

We have seen that the Kerr constant of the colloidal dispersion is made up of three contributions. The frequency-independent contribution, which is associated with an electronic polarization mechanism, contains information about the shape and the intrinsic anisotropy of the particle. The other two contributions are connected with the fact that the particle is a poly-ion. Following the standard view [12], we assume that counter-ions can be separated into two distinct categories: bound counter-ions (called condensed counter-ions by some authors) which are constrained to stay close

to the particle surface, and dissociated counter-ions which are spread over a distance of the order of the Debye-Hückel length. We suggest that the contribution present at very low frequencies, which becomes evident with the reversing-pulse technique, arises from a fluctuating electric dipole originating from the dynamics of bound counter-ions. The contribution which gives the frequency dispersion of B/Φ shown in figures 4 and 5 is instead connected with the existence of the cloud of dissociated counter-ions. As shown by the data of figure 6, this latter effect is predominantly collective, that is, it becomes important when there is an appreciable overlap of the counter-ion clouds belonging to different particles.

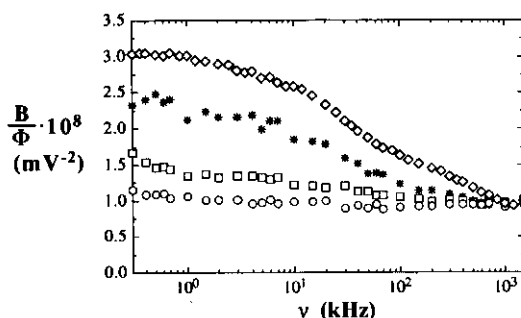


Figure 5. The specific Kerr constant measured as a function of the frequency of the electric field, at $\Phi = 1.5\%$, for four distinct concentrations of added NaCl: \diamond , $c_s = 0$ mM; *, $c_s = 0.2$ mM; \square , $c_s = 1$ mM; \circ , $c_s = 5$ mM.

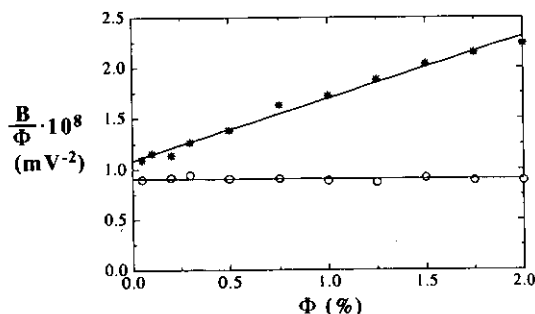


Figure 6. The specific Kerr constant measured as a function of the volume fraction, at $c_s = 0.2$ mM, for two distinct frequencies of the electric field: *, $\nu = 2.5$ kHz; \circ , $\nu = 1$ MHz.

3.1. Particle anisotropy

We recall that the existence of a non-zero Kerr constant implies the simultaneous presence in the particle of an electrical anisotropy (which produces the orientation of the particle when the electric field is applied) and of an optical anisotropy (which

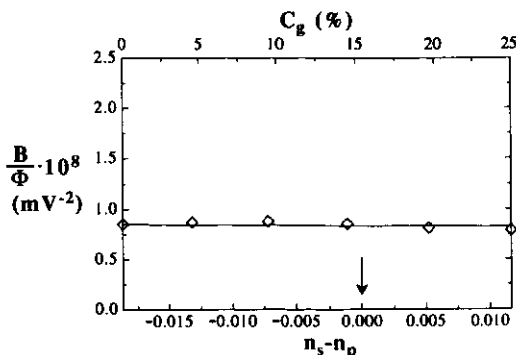


Figure 7. The specific Kerr constant measured as a function of the optical mismatch between particle and solvent. The upper abscissa scale reports the weight fraction of glycerol in water.

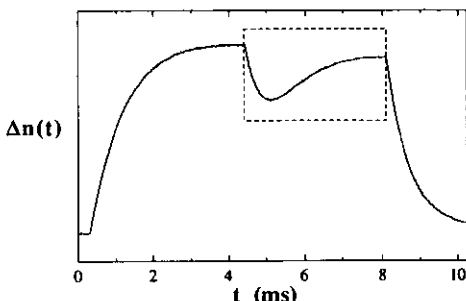


Figure 8. The electric birefringence response to a reversing-field pulse, at $c_s = 0.2$ mM and $\Phi = 0.1\%$.

allows the detection of the orientation of the particle by optical means). If the particles have a symmetry axis, the expression for the specific Kerr constant is [15]

$$B/\Phi' = [(n_s^2 + 2)^2/270V \lambda n_s \epsilon_0 k_B T](\alpha_1^o - \alpha_2^o)(\alpha_1^e - \alpha_2^e) \quad (1)$$

where α_1^o and α_1^e are, respectively, the optical and electrical polarizability of the particle along the symmetry axis, α_2^o and α_2^e are the polarizabilities perpendicular to the symmetry axis, V is the particle volume, and ϵ_0 the vacuum dielectric constant. If the particles possess both form and intrinsic anisotropy, we have [16]

$$(\alpha_1^e - \alpha_2^e) = V \epsilon_0 \epsilon_s \frac{\delta \epsilon_{int}/\epsilon_s + (L_2 - L_1)(\epsilon_1 - \epsilon_s)(\epsilon_2 - \epsilon_s)/\epsilon_s^2}{(1 + L_1(\epsilon_1 - \epsilon_s)/\epsilon_s)(1 + L_2(\epsilon_2 - \epsilon_s)/\epsilon_s)} \quad (2)$$

$$(\alpha_1^o - \alpha_2^o) = V \epsilon_0 n_s^2 \frac{(n_1^2 - n_s^2)/n_s^2 + (L_2 - L_1)(n_1^2 - n_s^2)(n_2^2 - n_s^2)/n_s^4}{(1 + L_1(n_1^2 - n_s^2)/n_s^2)(1 + L_2(n_2^2 - n_s^2)/n_s^2)} \quad (3)$$

where ϵ_s is the relative dielectric constant of the solvent, $\delta \epsilon_{int} = \epsilon_1 - \epsilon_2$ is the intrinsic electrical anisotropy, and L_1, L_2 are form factors which depend only on the particle geometry [19]. We recall that $L_1 + 2L_2 = 1$.

We know from our previous light scattering studies [13] that PFA particles possess an intrinsic optical anisotropy which derives from their partially crystalline internal structure. We may infer that the particles also have an intrinsic electrical anisotropy, $\delta\epsilon_{\text{int}} \cong 2n_p \delta n_{\text{int}} = 0.0138$. If we take the particles as perfectly spherical, we obtain from equations (1)–(3) a non-zero Kerr constant, but the value calculated from the known intrinsic anisotropy is much smaller than the measured value. In order to explain the experimental data it must be assumed that the actual particle shape is slightly different from spherical. Equations (2) and (3) can be simplified if we take into account that the particles have a refractive index very close to that of the solvent, while the static dielectric constant of the solvent is much larger than that of the particles ($\epsilon_1 \approx \epsilon_2 \approx 2$). This implies that the anisotropy of the electrical polarizability is essentially determined by the form of the particle and by the difference in dielectric constant with the solvent, while the optical part is dominated by the intrinsic anisotropy. The latter point is confirmed by the results shown in figure 7: we see that large relative variations of the difference between average refractive index of the particle and refractive index of the solvent have little effect on the high-frequency value of B/Φ . Taking into account all these considerations, we can approximate equation (2) by putting $\epsilon_1 = \epsilon_2 = \epsilon_p$, and equation (3) by putting $L_1 = L_2 = \frac{1}{3}$:

$$(\alpha_1^e - \alpha_2^e) = V\epsilon_0\epsilon_s \frac{(L_2 - L_1)(\epsilon_p - \epsilon_s)^2/\epsilon_s^2}{[1 + L_1(\epsilon_p - \epsilon_s)/\epsilon_s][1 + L_2(\epsilon_p - \epsilon_s)/\epsilon_s]} \quad (2')$$

$$(\alpha_1^o - \alpha_2^o) = V\epsilon_0n_s^2 \frac{(n_1^2 - n_2^2)/n_s^2}{[1 + (n_1^2 - n_2^2)/(3n_s^2)][1 + (n_2^2 - n_s^2)/(3n_s^2)]} \quad (3')$$

Modelling the particle as a prolate ellipsoid with semi-axes a, b, b , we get a fairly good agreement with the measured value of the Kerr constant if we take the value $a/b = 1.025$ for the ratio between the semi-axes. Such a slight ellipticity is consistent with a study of the particle shape based on the analysis of electron microscope pictures of the kind shown in figure 1.

It should be noted that a further assumption is needed to account for the experimental data: if there were no correlation between the direction of the geometrical axis and that of the optical axis of the particle, no electric birefringence could be expected. Indeed, averaging over all the particles would correspond to summing equal amounts of positive and negative birefringence contributions. So we assume that the two directions coincide (to account for the *positive* sign of the birefringence): this is a reasonable assumption if one considers that the direction of the optical axis coincides with the average direction of crystal growth [13], so that one may expect the particles to be slightly elongated along this direction.

Considering that the particle shape is only slightly different from spherical and that ϵ_p is much smaller than ϵ_s , equation (2') can be further approximated to a form which will become useful later on in this paper:

$$(\alpha_1^e - \alpha_2^e) \approx -\alpha_p 3f^2/10 \approx V\epsilon_0\epsilon_s 9f^2/20 \quad (2'')$$

where $\alpha_p = V\epsilon_0(\epsilon_p - \epsilon_s)[3\epsilon_s/(\epsilon_p + 2\epsilon_s)] \approx -1.5V\epsilon_0\epsilon_s$ is the particle excess polarizability with respect to the solvent, and $f^2 = 1 - (b/a)^2$.

3.2. Reversing-pulse data

A response of the kind shown in figure 8 could, at first sight, suggest that the particles possess a permanent dipole moment. Similar effects were detected in TMV [2], DNA [5], and NAPSS solutions [8], and a considerable debate exists in the literature concerning the possible existence of permanent electric dipoles in macro-ions [18]. It should be noted that what really matters in calculating the Kerr constant of the system is the average square value of the dipole moment. This means that, even with a zero average dipole moment, we can still have a contribution to the Kerr constant arising from fluctuations. The origin of the fluctuating electric dipole in a charged particle can be related to statistical fluctuations of the charge distribution on the surface, as it was proposed some time ago by Kirkwood and Shumaker to account for the dielectric response of globular proteins [20]. If the centre of charge does not coincide with the centre of mass for a given particle, an applied electric field will generate a torque tending to align along its direction the centre-of-charge displacement vector, and this is equivalent to the effect of an electric dipole moment. Since the position of bound counter-ions is fluctuating with time, the random dipole moment of the particle presents temporal fluctuations of zero average. We call τ_i the correlation time of such fluctuations. Earlier discussions have implicitly assumed that fluctuations of the charge distribution are completely unaffected by the applied field. South and Grant [21] included in their approach the fact that the bound counter-ions will tend to move in the direction of the field, and derived the following expression for the relaxation time τ of the polarizability contribution due to charge fluctuations:

$$1/\tau = 1/\tau_i + 1/3\tau_r. \quad (4)$$

As a first approximation, the act of positioning a given number of charges on the surface of a macro-ion can be regarded as a point process, obeying essentially Poisson statistics. Assuming that each charge will take a random position on the spherical particle of radius R , it is easy to calculate that, for Z monovalent charges, the mean square displacement of the centre of charge from the centre of mass of the particle will be simply R^2/Z . As a consequence, the mean square value of the fluctuating dipole is $\langle \delta\mu^2 \rangle = e^2 Z R^2$. A similar expression is given by Kirkwood and Shumaker [20]. The effect of charge fluctuations is that of generating a contribution to the polarizability of the particle, which can be expressed as [21]

$$\alpha_c = \langle \delta\mu^2 \rangle / k_B T. \quad (5)$$

Obviously, if the particles were perfect spheres, the charge displacement vector would be randomly directed with respect to the anisotropy axis, so that, by averaging over all particles, we would not obtain any dependence of the induced birefringence on the sign of the field. In order to calculate the steady-state contribution of α_c to the electrical anisotropy, we can proceed in a way similar to that followed in the derivation of equation (2''), and assume that the contribution of charge fluctuations to the electrical anisotropy is simply obtained by multiplying α_c by the same factor $3f^2/10$ which appears in equation (2'').

If the particles have cylindrical symmetry and a fluctuating dipole moment, the rise of induced birefringence following the application of a stepwise electric field at $t = 0$ is given by [8]

$$\Delta n_{\text{rise}} / \Delta n_s = 1 - A \exp(-t/\tau) - (1 - A) \exp(-t/\tau_r) \quad (6)$$

where Δn_s is the steady-state birefringence, and

$$A = S\tau / (S + 1)(\tau - \tau_r) \quad (7)$$

with

$$S = \langle \delta\mu^2 \rangle / \alpha_p k_B T = \alpha_c / \alpha_p. \quad (8)$$

If a field reversal is performed at $t = t_0$, with t_0 much larger than τ_r and τ , the induced birefringence response is [8]

$$\Delta n_{\text{rev}} / \Delta n_s = 1 - 2A \{ \exp[-(t - t_0)/\tau] - \exp[-(t - t_0)/\tau_r] \}. \quad (9)$$

Note that, if $\tau_i \rightarrow \infty$, then $\tau = 3\tau_r$, and equations (4) and (9) take the form expected for particles possessing a permanent dipole moment. The decay of the induced birefringence after the switch-off of the field at $t = 2t_0$ is given by

$$\Delta n_{\text{decay}} / \Delta n_s = \exp[-(t - 2t_0)/\tau_r]. \quad (10)$$

Equations (6), (9) and (10) are in agreement with equation (48) of [22] which connects the three birefringence transients in a general relation.

It is useful to generalize equation (9) to the case in which the field is E' before reversal and E after reversal, with E not necessarily equal to $-E'$. We have derived the expression for the transient due to a sudden change, at the instant $t = 0$, of the field from E' to E , by assuming that $\Delta n(0)$ coincides with the steady-state value due to E' :

$$\Delta n(t) = \Delta n_s [1 + L \exp(-t/\tau_r) + M \exp(-t/\tau)] \quad (11)$$

where $L = (r^2 - 1) - M$, $M = (r - 1)A$, and $r = E'/E$. The symmetric field reversal corresponds to the case $r = -1$, which means $L = -M$, and $M = -2A$. In our experiment the setting of r was close to -1 within a few per cent, but even a 1% variation of r has important effects on the shape of the dip. We have therefore used equation (11) in order to fit the experimental dip with free parameters r , S and τ , taking for τ_r the value derived from the fit of the pulse decay after the switch-off of the electric field. We find $S = 0.5 \pm 0.1$ and $\tau = (610 \pm 30) \mu\text{s}$. An example of the quality of the fit is shown in figure 9. The full curve is the fitting curve with parameters $r = -1.03$, $S = 0.56$ and $\tau = 600 \mu\text{s}$. We note that τ is much shorter than the value $3\tau_r$, which one would find with particles having a true permanent dipole. The broken curve in figure 9 gives, for the sake of comparison, the time behaviour of the dip which would be expected for the case of a permanent dipole moment. By using equations (4) and (8), we can derive from the best-fit parameters the values $\tau_i = (1000 \pm 100) \mu\text{s}$ and $\langle \delta\mu^2 \rangle^{1/2} = (7.9 \pm 1) \times 10^{-26} \text{ C m}$.

All the dips we have observed for changing the concentration of added salt in the range 0–3 mM can be fitted, within experimental error, with the same parameters S and τ . Although we did not make a systematic study of the Φ -dependence of the dip, the available data indicate also that both S and τ are not affected by changes of the particle volume fraction.

In principle, S and τ could have been derived without field-reversal by simply comparing the rise and decay of the EB response to a rectangular electric field pulse.

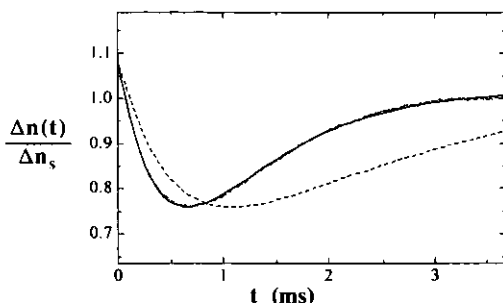


Figure 9. An enlarged view of the dip shown in figure 8. The full curve representing the best-fit curve (equation (11)), is almost indistinguishable from the experimental data. The broken curve gives the behaviour expected for a particle having a permanent dipole.

Indeed we have observed in our experiment that the rise of the induced birefringence is slower than the decay and is non-exponential. However, the uncertainty in the determination of the fitting parameters becomes much larger than that of the field reversal experiment, because the rise (see equation (6)) contains the sum of two exponentials having similar time constants, whereas the response to field reversal (see equation (9)) contains the difference between the same exponentials.

The relaxation time of the fluctuating dipole arises from the displacement of bound but mobile counter-ions along the particle surface. The translational diffusion of the tightly bound counter-ions is expected to be much slower than that of free counter-ions. If we write τ_i as $\tau_i \approx R^2/D_b$, where D_b is the translational diffusion constant of bound counter-ions, we obtain from our data $D_b \approx 10^{-7} \text{ cm}^2 \text{ s}^{-1}$ which is two orders of magnitude smaller than that of free ions in water, and is rather close to the value derived by Ookubo *et al* [8] in the case of flexible polyelectrolyte solutions.

In order to compare the best-fit value of $\langle \delta\mu^2 \rangle^{1/2}$ with the predicted value, we should not take for Z the total structural charge Z_s , but rather the renormalized effective charge [23] that may be attributed to the particle when counter-ion condensation is taken into account. According to [22], the approximate value for the renormalized charge of a spherical particle is $Z \approx 6R/L_B$, $L_B = e^2/(4\pi\epsilon_0\epsilon_s k_B T)$ being the Bjerrum length (about 0.7 nm for water solutions). We find that the expression $\langle \delta\mu^2 \rangle^{1/2} = eR\sqrt{Z}$ considerably overestimates the root-mean-square fluctuating dipole. This is not surprising because the assumption that the charges are randomly distributed over the particle surface is not realistic, and any model which would impose a constraint on the minimum distance among charged sites would predict a lower value for $\langle \delta\mu^2 \rangle^{1/2}$.

It should be recalled that, independently from [19], Mandel [24] calculated α_c several years ago, by assuming that fluctuations are negligible and that the electric dipole is induced by the field through a slight displacement of bound counter-ions from their equilibrium position. Several authors [12] have subsequently modified the approach of [24] by introducing into the expression for α_c some dependence on the ionic strength of the solution. Apart from the fact that Mandel's formula refers to a long rod-like macromolecule instead of a spherical particle, the main difference with the formula used by us is that the expression of [24] contains, instead of Z , the number of bound counter-ions, which is given by $Z_s - Z$. The available experimental data on the effective charge of spherical macro-ions [25, 26] seem to support the

theory of charge renormalization [23], and indicate that Z can be considerably smaller than Z_0 , so that Mandel's formula predicts values of α_c which are much larger than those predicted by our formula and, therefore, make the agreement with our experimental data even worse. Concerning the response to field reversal, the dip shown in figure 9 could probably be equally well described by using the hypothesis of a slow induced dipole.

Another point to stress is our experimental observation that the amplitude of the dip does not depend on the concentration of added salt in the range 0–3 mM. This shows that α_c is not appreciably influenced by the ionic strength, in contrast with the theories mentioned above [12].

We have no evidence of interparticle interaction effects on the amplitude of the fluctuating dipole contribution: indeed, the dip looks less pronounced at high volume fractions, but this is simply explained by the relative increase of the contribution due to the undissociated counter-ions.

3.3. Collective effects

The data reported in figures 6–8 show that, besides the effects arising from the intrinsic properties of the particles and from charge fluctuations, there is an additional contribution to the Kerr constant of the dispersion which presents the following features:

(i) it contains a term proportional to Φ^2 whereas single-particle effects are proportional to Φ ;

(ii) it is strongly dependent on the concentration of added salt; and

(iii) it is a decreasing function of the frequency of the applied field.

The first two features clearly indicate that the effect depends on the overlap of the counter-ion clouds surrounding each particle: when the overlap is reduced, either by increasing the ionic strength or by decreasing the particle concentration, the effect disappears. We have already reported a similar observation from a TEB experiment on dispersions of rod-like polytetrafluoroethylene latex particles [4].

Since the limit value of B/Φ at low frequency for vanishing volume fraction is almost coincident with the high-frequency value, we have to conclude that undissociated counter-ions contribute only slightly to the polarizability in the single-particle limit. No theory of polyelectrolyte solutions which takes into account interparticle interactions seems to be available. Unfortunately, all the treatments of counter-ion polarizability are essentially single-particle approaches.

We have tried a mean-field approach to interparticle interactions [27]: if the effect of interactions is that of modifying the local field that a particle effectively feels, we can tentatively assume that the specific Kerr constant can still be calculated with equations (1)–(3) by simply using, instead of the relative dielectric constant of the solvent, the relative dielectric constant of the solution, ϵ_{sol} . It should be noted that, if we use the approximated expression given by equation (2'') for the electrical anisotropy, we find that B/Φ is proportional to the relative dielectric constant of the solvent. Therefore, the proposed mean-field approach implies that, for our system, B/Φ should be approximately proportional to the dielectric constant of the solution. Many theoretical papers [28–30] have been devoted to the calculation of ϵ_{sol} for spherical macro-ions. At low volume fractions and under the approximation that the ratio between the Debye–Hückel length l_{DH} and the particle radius is small, ϵ_{sol} can be expressed as [28–30]

$$\epsilon_{\text{sol}} = \epsilon_s [1 + k\Phi F(\omega)] \quad (12)$$

where k depends on the particle properties and on the ionic strength of the solution, and $F(\omega)$ is given by

$$F(\omega) = 1/(1 + \omega^{1/2}\tau_s^{1/2})(1 + \omega\tau_s) \quad (13)$$

where $\omega = 2\pi\nu$ and τ_s is a relaxation time which is given by $\tau_s = R^2/(2D)$ [28–30], D being the diffusion coefficient of the undissociated counter-ions.

If B/Φ is proportional to ϵ_{sol} , equation (12) can explain the observed linear dependence of B/Φ on Φ (see figure 6). We will report on a detailed study of the behaviour of the slope k as a function of the ionic strength in a separate paper. The frequency dependence of the Kerr constant is markedly non-Lorentzian, as shown in figure 10. We find a very good fit with the function $F(\omega)$, with the best-fit value $\tau_s = 1.9 \mu\text{s}$. Note that τ_s is much smaller than τ_i . This is reasonable because $D \gg D_b$. It should be added that both the shape of the curve and the value of τ_s are not influenced by changes of c_s and Φ in the investigated range of parameters.

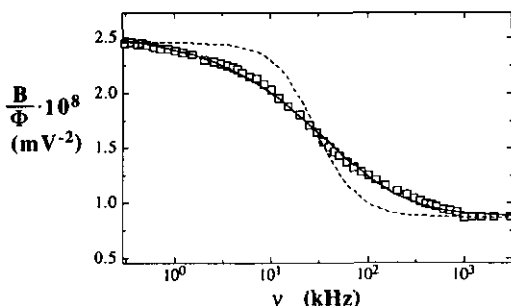


Figure 10. The specific Kerr constant measured as a function of the frequency of the electric field, at $c_s = 0.2 \text{ mM}$ and $\Phi = 2.5\%$. The full curve represents the fit with equation (13), the broken curve shows a Lorentzian fit.

In our case, at $c_s = 0.2 \text{ mM}$, l_{DH} is about 22 nm. Although equation (12) is derived under the approximation $l_{\text{DH}}/R \ll 1$, it is possible that its validity is not limited to the range of very small l_{DH}/R .

4. Conclusions

We have shown in this paper that fluorinated latex (PFA) particles represent a very interesting model system for TEB studies of the dielectric properties of polyelectrolytes. The specific Kerr constant of the particle dispersion is rather large because the particles possess both an intrinsic optical anisotropy and a slightly elliptical average shape.

The reversing-pulse technique gives a TEB response which is interpreted as due to a fluctuating electric dipole. The existence of the dipole arises from the fact that the instantaneous charge distribution on the particle surface is not centrosymmetric. The dipole fluctuates with time because the position of bound counter-ions changes

with time. We have derived the lifetime τ_i of dipole fluctuations. We have also found that both $\langle \delta\mu^2 \rangle$ and τ_i are rather insensitive to salt addition and to variations of the particle volume fraction.

The specific Kerr constant presents a contribution whose amplitude is strongly dependent on both particle and salt concentration. The frequency dispersion of such a contribution is markedly non-Lorentzian, and fits the predicted frequency dispersion for the dielectric constant of the solution very well. A simple mean-field argument is used to justify this latter result.

Acknowledgments

We thank D Lenti for the gift of the Hyflon latex particles, and T Bellini for useful comments. The TEM picture reported in figure 1 was taken with the kind collaboration of M Walet at DSM Research, Netherlands. We acknowledge financial support from MURST 40%.

References

- [1] O'Konsky C T and Haltner A J 1956 *J. Am. Chem. Soc.* **78** 3604
- [2] Newman J and Swinney H L 1976 *Biopolymers* **15** 301
- [3] Thurston G B and Bowling D I 1969 *J. Colloid Interface Sci.* **30** 34
- [4] Bellini T, Piazza R, Sozzi C and Degiorgio V 1988 *Europhys. Lett.* **7** 561
- [5] Elias J G and Eden D 1981 *Macromolecules* **14** 410
Hans M and Bernengo J C 1973 *Biopolymers* **12** 2151
- [6] Wijnenga S S and Mandel M 1988 *J. Chem. Soc. Faraday Trans. 1* **84** 2483
- [7] Tricot M and Houssier C 1982 *Macromolecules* **15** 854
- [8] Ookubo N, Teraoka I and Hayakawa R 1988 *Ferroelectrics* **86** 19
- [9] Ookubo N, Hirai Y, Ito K and Hayakawa R 1989 *Macromolecules* **22** 1359
- [10] Degiorgio V, Bellini T, Piazza R, Mantegazza F and Goldstein R E 1990 *Phys. Rev. Lett.* **64** 1043
- [11] Krämer U and Hoffmann H 1991 *Macromolecules* **24** 256
- [12] Mandel M and Odijk T 1984 *Ann. Rev. Phys. Chem.* **35** 75
- [13] Piazza R, Stavans J, Bellini T, Lenti D, Visca M and Degiorgio V 1990 *Prog. Colloid Polymer Sci.* **81** 89
Piazza R and Degiorgio V 1992 *Opt. Commun.* **92** 45
- [14] Piazza R, Degiorgio V and Bellini T 1986 *J. Opt. Soc. Am. B* **3** 1642
- [15] Fredericq E and Houssier C 1973 *Electric Dichroism and Electric Birefringence* (Oxford: Clarendon)
- [16] O'Konski C T (ed) 1976 *Molecular Electro-optics* (New York: Dekker)
- [17] Jennings B R (ed) 1979 *Electro-optics and Dielectrics of Macromolecules and Colloids* (New York: Plenum)
- [18] Stoylov S P 1991 *Colloid Electro-optics: Theory, Techniques, Applications* (London: Academic)
- [19] van de Hulst H C 1981 *Light Scattering by Small Particles* (New York: Dover)
- [20] Kirkwood J G and Shumaker J B 1952 *Proc. Natl Acad. Sci., US* **38** 855
- [21] South G P and Grant E H 1973 *Biopolymers* **12** 1937
- [22] Matsumoto M, Watanabe H and Yoshioka K 1970 *J. Phys. Chem.* **74** 2182
- [23] Alexander S, Chaikin P M, Grant P, Morales G J, Pincus P and Hone D 1984 *J. Chem. Phys.* **80** 5776
Belloni L 1985 *Chem. Phys.* **99** 43
- [24] Mandel M 1961 *Mol. Phys.* **4** 489
- [25] Ookubo T 1988 *J. Colloid Interface Sci.* **125** 380
- [26] Bucci S, Fagotti C, Degiorgio V and Piazza R 1991 *Langmuir* **7** 824
- [27] Bellini T 1990 *PhD Thesis* Università di Pavia
- [28] Fixman M 1980 *J. Chem. Phys.* **72** 5177
- [29] Chew W C and Sen P N 1982 *J. Chem. Phys.* **77** 4683
- [30] Vogel E and Pauly H 1988 *J. Chem. Phys.* **89** 3823